6

Wavelet Expansions

6.1 THE CONTINUOUS WAVELET TRANSFORM

The continuous wavelet transform (CWT) is defined by

$$X(b,a) = \frac{1}{\sqrt{|a|}} \int_{-\infty}^{\infty} x(t)\overline{\psi(\frac{t-b}{a})}dt \tag{6.1}$$

One interpretation of the transform $X(b,a)$ is that it provides a measure of similarity between the signal $x(t)$ and the continuously translated and dilated *mother wavelet* $\psi(t)$. The inverse wavelet transform is then provided by

$$x(t) = \frac{1}{\sqrt{|a|}C_\psi} \int_{-\infty}^{\infty}\int_{-\infty}^{\infty} X(b,a)\psi(\frac{t-b}{a})\frac{dadb}{a^2} \tag{6.2}$$

where $\mathcal{F}(\psi(t)) = \tilde{\psi}(\omega)$ and

$$C_\psi = \int_{-\infty}^{\infty} \frac{|\tilde{\psi}(\omega)|^2}{|\omega|}d\omega \tag{6.3}$$

Together, equations (6.1) and (6.2) form the continuous wavelet transform pair.

For the inverse transform to exist, it is required that the *admissibility condition* $C_\psi < \infty$ be satisfied. The value C_ψ will in general not be finite if the integrand blows up at $\omega = 0$. Hence it is required that

$$\tilde{\psi}(0) = 0 \tag{6.4}$$

(Recall that $\psi(t) \in L^1(\mathbb{R})$ implies that $\tilde{\psi}(\omega)$ is continuous.) If this condition is only satisfied approximately, i.e., $\tilde{\psi}(0) \approx 0$, then it is said to be *almost* admissibile. For example, the Morlet wavelet is almost admissible. The admissibility requirement given by Equation 6.4, may be interpreted further by inverting the Fourier transformation. Recall that

$$\tilde{\psi}(\omega) = \int_{-\infty}^{\infty} \psi(t)e^{-i\omega t}dt$$

Substituting $\omega = 0$ into the above results in

$$\int_{-\infty}^{\infty} \psi(t) = 0 \tag{6.5}$$

So admissible mother wavelets have zero mean.

For future reference we define the scaled and translated window

$$g_{ab}(t) = \frac{1}{\sqrt{|a|}}\psi(\frac{t-b}{a})$$

where a is the *scale* parameter and b is the *shift* parameter. The factor $1/\sqrt{|a|}$ ensures that the window is normalized at all scales, i.e.,

$$\|\psi(t)\|^2 = 1, \quad \Rightarrow \quad \|g_{ab}(t)\|^2 = 1 \tag{6.6}$$

See Figure 6.1 for a display of the dilated and shifted Gaussian window.

Properties of the Continuous Wavelet Transform

We may denote the CWT transform pair either as

$$\mathcal{W}(x(t)) = X(b,a)$$

or as

$$x(t) \leftrightarrow X(b,a)$$

Property 6.1.1. *Linearity of the CWT.*

$$\mathcal{W}(x(t)+y(t)) = \mathcal{W}(x(t)) + \mathcal{W}(y(t)) \tag{6.7}$$

$$\mathcal{W}(cx(t)) = c\mathcal{W}(x(t)) \tag{6.8}$$

Property 6.1.2. *Shifting Property.*

$$x(t) \leftrightarrow X(b,a) \tag{6.9}$$

$$x(t-t_0) \leftrightarrow X(b-t_0,a) \tag{6.10}$$

Property 6.1.3. *Scaling Property.*

$$x(\frac{t}{\alpha}) \leftrightarrow \sqrt{\alpha}X(\frac{b}{\alpha},\frac{a}{\alpha}) \tag{6.11}$$

Property 6.1.4. *Energy Property*

$$\int_{-\infty}^{\infty} x(t)\overline{y(t)}dt = \frac{1}{C_\psi}\int_{-\infty}^{\infty}\int_{-\infty}^{\infty} X(b,a)\overline{Y(b,a)}\frac{dadb}{a^2} \tag{6.12}$$

Property 6.1.5. *Linearity of the Wavelet. If the collection of functions* $\{\psi_i(t)\}$ *are wavelets, i.e., they satisfy the admissibility condition, then the linear combination*

$$\psi(t) = \sum_i c_i\psi_i(t)$$

is also a wavelet (since it also satisfies the admissibility condition). See [82].

Wavelet Analysis in the Fourier Domain

It will be useful to know that the Fourier transform of the scaled and dilated mother is given by

$$g_{ab}(t) = \frac{1}{\sqrt{|a|}}\psi(\frac{t-b}{a}) \leftrightarrow \sqrt{|a|}e^{-ib\omega}\tilde{\psi}(a\omega) = G_{ab}(\omega) \tag{6.13}$$

In addition, the Fourier transform of the forward CWT is found using Parseval's equation, i.e.,

$$X(b,a) = (x(t), g_{ab}(t)) \tag{6.14}$$

$$= \frac{1}{2\pi}\int_{-\infty}^{\infty} X(\omega)\overline{G_{ab}(\omega)}d\omega \tag{6.15}$$

Substituting Equation (6.13) into the above gives the desired representation of the CWT in the Fourier domain

$$X(b,a) = \frac{\sqrt{|a|}}{2\pi}\int_{-\infty}^{\infty} X(\omega)\overline{\tilde{\psi}(a\omega)}e^{i\omega b}d\omega \tag{6.16}$$

6.1.1 Interpretting the CWT

In contrast to the STFT which produced a transformation of data to the time-frequency domain (τ,ω), the wavelet transform transforms time-scale plane (b,a). In the former case, it is standard to examine the graph of the magnitude of the STFT $|X(\tau,\omega)|$. This time-frequency diagram is referred to as the spectrogram. In the latter case, the spectrogram is replaced by the *scalogram* which consists of the graph of the magnitude of the CWT, i.e., $|X(b,a)|$. In both cases there is an associated phase diagram, e.g., the polar form of the CWT is

$$X(b,a) = |X(b,a)|e^{\phi(b,a)}$$

Note also that both the STFT and the CWT map a 1-dimensional signal to a 2-dimensional representation.

In what follows we consider *localization* features of the CWT which aid in the interpretation of the scaleogram. Our presentation follows [26].

Time-Localization of the CWT.

For the moment, we assume that the wavelet $\psi(t)$ vanishes identically outside the time domain $[t_{\min}, t_{\max}]$ where $t_{\min} < 0$ and $t_{\max} > 0$. Although this condition may not be true in practice, the magnitude of the wavelet will in general be very small, and approximately zero on this interval.

$X(b,a)$ dependence on t_0. We define the domain of influence of the signal $x(t)$ at the point $t = t_0$ to be the region in the (b,a)-plane such that the values of $X(b,a)$ are dependent on t_0.

To demonstrate the time-localization property of the CWT we consider the signal $x(t) = \delta(t - t_0)$. Substituting this choice for $x(t)$ into equation (6.1) gives

$$X(b,a) = \frac{1}{\sqrt{|a|}}\int_{-\infty}^{\infty}\delta(t-t_0)\overline{\psi(\frac{t-b}{a})}dt$$

which integrates to

$$X(b,a) = \frac{1}{\sqrt{|a|}}\overline{\psi(\frac{t_0-b}{a})}$$

Note that $\overline{\psi(\frac{t_0-b}{a})} = 0$ unless

$$\frac{t_0-b}{a} \in [t_{\min}, t_{\max}]$$

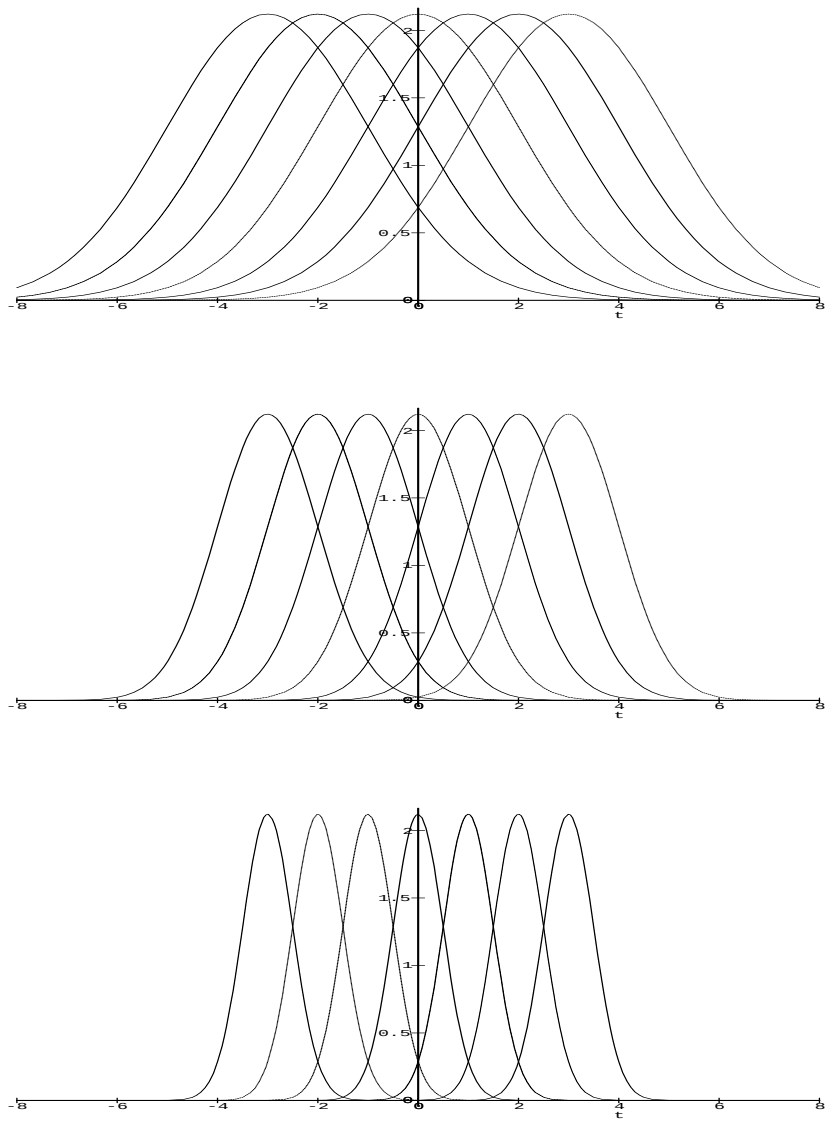

Fig. 6.1 This figure displays dilations and shifts of the Gaussian window $\psi((t-b)/a)$ for discrete values of $b = -3, -2, -1, 0, 1, 2, 3$. Top: The dilation corresponding to $a = 2$. Middle: $a = 1$. Bottom: $a = 1/2$.

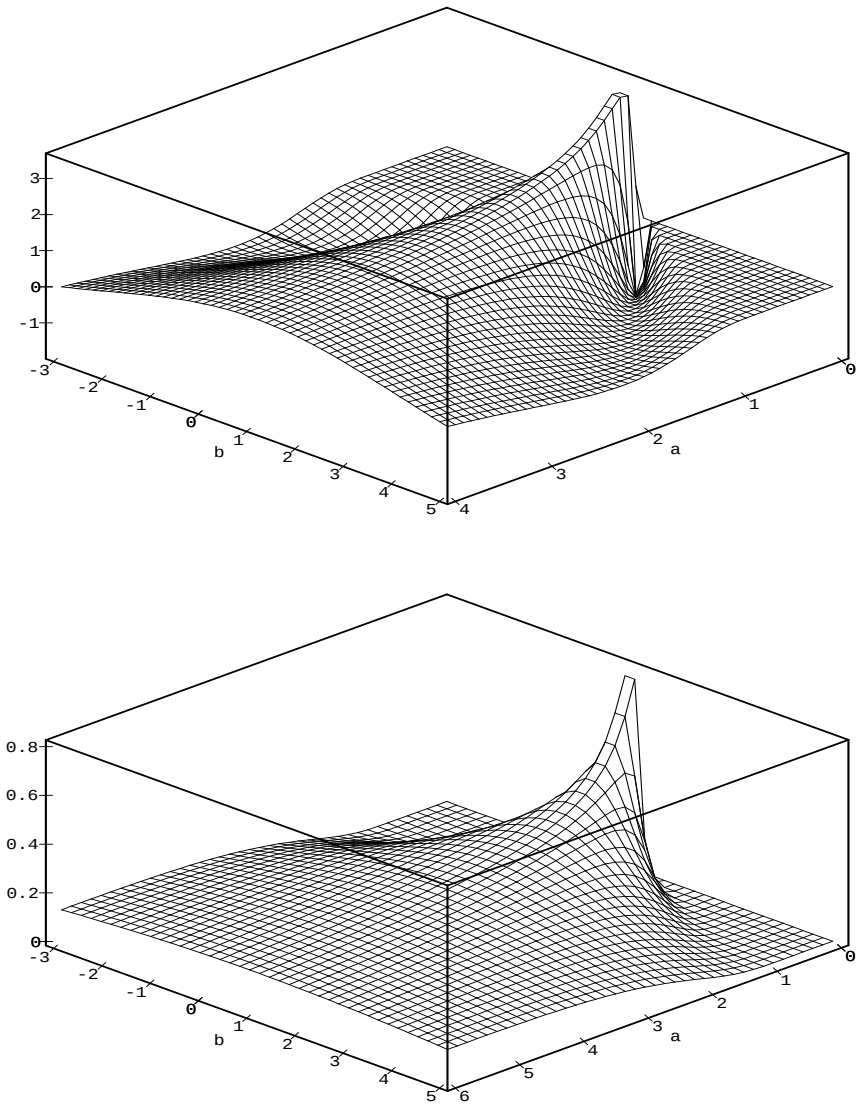

Fig. 6.2 Top: The scalogram of the Mexican hat wavelet transform of the delta function centered at $t = 1$. Bottom: The scalogram of the Morlet wavelet transform of the same delta function.

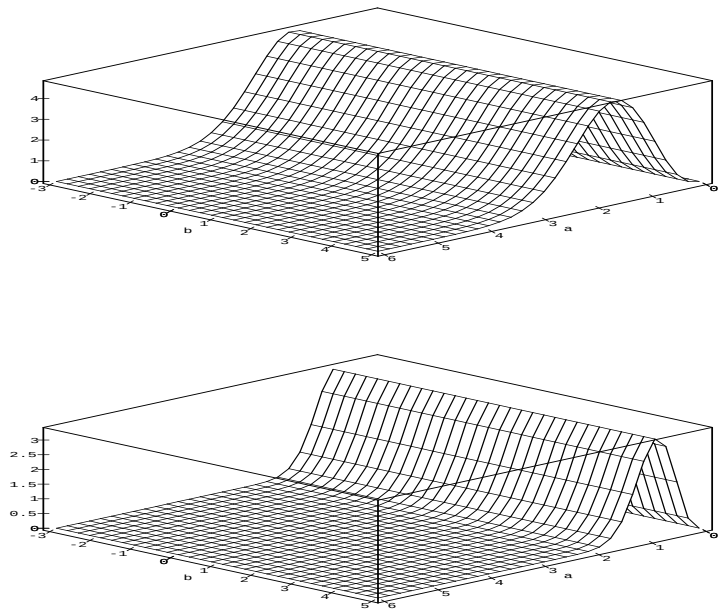

Fig. 6.3 Top: The scalogram of the Mexican hat wavelet transform of the monochromatic complex exponential $x(t) = \exp(it)$. Bottom: The scalogram of the Mexican hat wavelet transform of the monochromatic complex exponential $x(t) = \exp(i2t)$.

This condition defines 2 lines, $at_{\min} + b = t_0$ and $at_{\max} + b = t_0$, which intersect at the point t_0 and delimit the region in the (b,a) plane for which the transform $X(b, a)$ depends on t_0. This situation is depicted in Figure 6.4.

The CWT $X(b, a)$ of the delta function $\delta(t - 1)$ is shown in Figure 6.2 for both the mexican hat wavelet and the Morlet wavelet. Observe that the width of the transform is narrower for smaller scale parameter a. The projection of the non-zero values of this transform fall into the domain of influence of the pulse originating at $t = 1$.

$X(b_0, a_0)$ dependence on t. Another helpful question to consider is for which values of t does the signal $x(t)$ contribute to the value of $X(b, a)$ at the point (b_0, a_0)? By examining Figure 6.4 we conclude that if

$$a_0 t_{\min} + b_0 \leq t \leq a_0 t_{\max} + b_0$$

then the value of $x(t)$ may influence the CWT at the point (b_0, a_0).

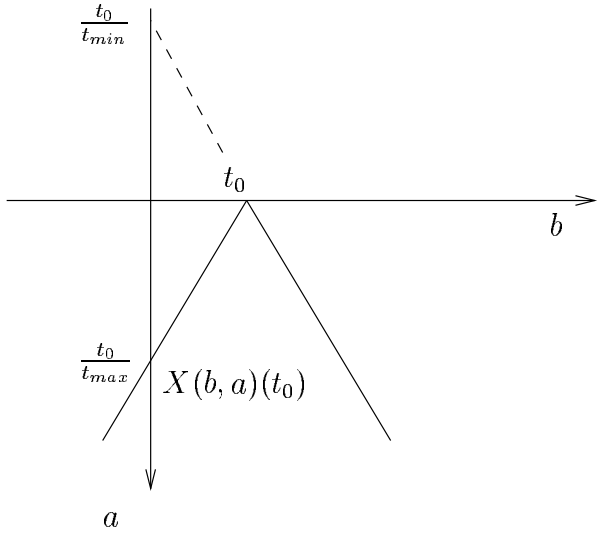

Fig. 6.4 The triangular region is the domain of influence of the point t_0 on the continuous wavelet transform $X(b,a)$

Frequency-Localization of the CWT.

In the previous section we considered the how a localized signal $x(t)$ in the time domain could influence the the values of the CWT $X(b,a)$. Now we examine the same question but focus on the influence of a pure sinusoid on the transform.

$X(b,a)$ dependence on ω_0. Now we consider for which portion of the (b,a) plane the CWT $X(b,a)$ is influenced by the frequency ω_0. To examine this let $x(t) = \exp(i\omega_0 t)$, the complex monochromatic signal with frequency ω_0. Given that the Fourier transform of $\exp(i\omega_0 t)$ is $2\pi\delta(\omega-\omega_0)$ we may compute the CWT of $x(t)$ using equation (6.16), i.e.,

$$X(b,a) = \frac{\sqrt{|a|}}{2\pi}\int_{-\infty}^{\infty} 2\pi\delta(\omega-\omega_0)\overline{\tilde{\psi}(a\omega)}e^{i\omega b}d\omega$$

from which we conclude that

$$X(b,a) = \sqrt{|a|}\overline{\tilde{\psi}(a\omega_0)}e^{i\omega_0 b}$$

If we now assume that the Fourier transform of the wavelet is band-limited, i.e., $\overline{\tilde{\psi}(\omega)} = 0$ whenever $\omega \notin [\omega_{\min}, \omega_{\max}]$. Hence, in general,

$$\tilde{\psi}(a\omega_0) = 0 \quad \text{if} \quad \omega_0 \in [\frac{\omega_{\min}}{a}, \frac{\omega_{\max}}{a}]$$

Fig. 6.5 The domain of influence for the monochromatic signal $x(t) = \exp(i\omega_0 t)$. Note that higher frequencies influence fewer coefficients.

Hence,

$$X(b,a) = 0 \quad \text{unless} \quad \omega_0 \notin [\frac{\omega_{\min}}{a}, \frac{\omega_{\max}}{a}]$$

In other words, the domain of influence of ω_0 on $X(b,a)$ is the horizontal strip defined by

$$\frac{\omega_{\min}}{\omega_0} \leq a \leq \frac{\omega_{\max}}{\omega_0} \tag{6.17}$$

The larger the value of ω_0, i.e., the higher the frequency of the monochromatic signal, the smaller the region of influence; see Figure 6.5.

The actual CWT of $\exp(i\omega_0 t)$ using the Mexican hat wavelet is shown in Figure 6.3 for 2 different values of ω_0. Compare this with Figure 6.6 which displays the CWT of the signal $\sin(\omega_0)$. The magnitude is no longer constant along lines a =constant. This effect can be problematic when interpreting scalograms. However, it may be avoided by employing *progressive* wavelets; see Problem 6.7 and reference [26] for further details.

It is also interesting to note that the actual value of a for which $|X(b,a)|$ is a maximum (see Figure 6.3) when the signal has the form $\exp(i\omega_0 t)$ is wavelet

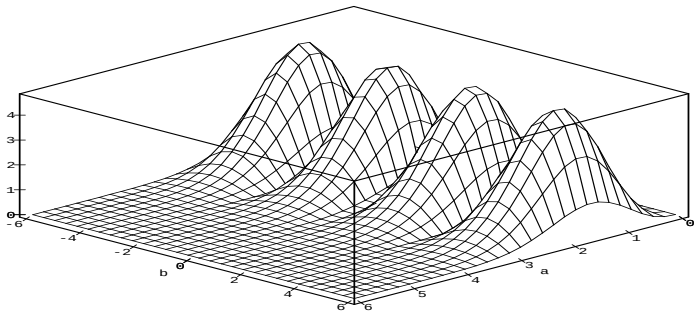

Fig. 6.6 The scalogram of the Mexican hat wavelet transform of the monochromatic signal $x(t) = \sin(t)$.

dependent. For instance, for the Mexican hat wavelet this value is

$$a = \frac{1}{\omega_0}\sqrt{\frac{5}{2}} \tag{6.18}$$

while for Morlet's wavelet

$$a = \frac{1}{2\omega_0}(\alpha + \sqrt{\alpha^2 + 2}) \tag{6.19}$$

See Problem 6.6 for more details.

$X(b_0, a_0)$ dependence on ω. Finally, it may be similarly argued that the Fourier components ω of $X(\omega)$ which influence the value of the CWT at the point (b_0, a_0) are determined by the relation

$$\frac{\omega_{\min}}{a_0} \leq \omega \leq \frac{\omega_{\max}}{a_0} \tag{6.20}$$

We observe that the bandwidth of the frequencies which influence $X(b, a)$ increases as the scale a decreases.

6.1.2 Discretization of the CWT

The number of instances for which the CWT of a signal may be computed analytically is obviously very small. In general, the evaluation of the CWT pair is done at a discrete set of points. In this Section we consider the discretization of the (b, a)-plane. Using the terminolgy of [26], we consider the

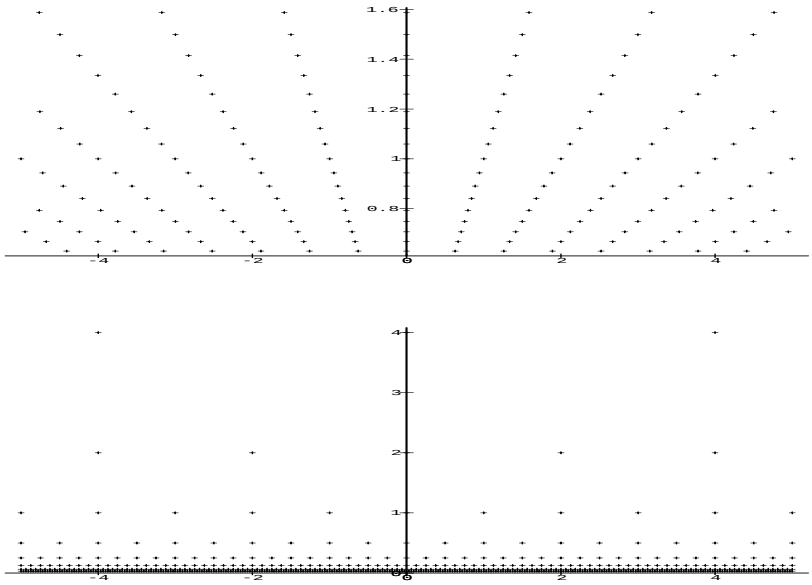

Fig. 6.7 Top: The sampling grid in the (b, a)-plane corresponding to $\alpha = 2^{1/12}, \beta = 1$. Middle: The dyadic sampling grid with $\alpha = 2, \beta = 1$.

restriction of $X(b, a)$ to a collection of fixed values, or *voices* a_j

$$a_j = \alpha^j \quad \text{where} \quad \alpha > 1 \quad \text{and} \quad j \in \mathbb{Z} \tag{6.21}$$

Observe that the width of the function $\psi((t-b)/\alpha^j)$ is dependent on the magnitude of α^j. In fact it is α^j times wider the mother wavelet, i.e.,

$$\operatorname{supp} \psi(\frac{t-b}{\alpha^j}) = \alpha^j \operatorname{supp} \psi(t)$$

This fact must be taken into account when discretizing the shift variable b.

The discretized shift size should be proportional to the width of the dilated wavelet. This may be accomplished by taking

$$b_k^j = k\beta\alpha^j \text{ where } \beta > 0 \tag{6.22}$$

Putting this all together we write the wavelet on the discretized grid as

$$\psi_k^j(t) = \alpha^{-\frac{j}{2}} \psi(\alpha^{-j}t - k\beta)$$

Then the discretized wavelet coefficient from Equation (6.1) is

$$X(b_k, a_j) = 2^{-j/2} \int_{-\infty}^{\infty} x(t)\overline{\psi(2^{-j}t - k)}dt \tag{6.23}$$

Example 6.1. Let $\alpha = 2^{1/l}$. The positive integer l is often referred as the number of voices per octave. A choice of $l = 12$ represents a fine sampling of the (b,a)-plane. See the top of Figure 6.7. The choice of discrete time shift β depends heavily on the nature of the data but typical values are between .1 and 1.

Example 6.2. Another importany choice of voice for the discrete grid is $\alpha = 2$ and $\beta = 1$. This coarser sampling of the (b,a)-plane produces a *dyadic* grid. See the bottom of Figure 6.7. It is also often convenient to display the grid using the coordinates $(b, -\ln a)$.

6.2 THE DISCRETE WAVELET TRANSFORM

Wavelet expansions are *local* expansions of the form

$$f(x) = \sum_{j=-\infty}^{\infty} \sum_{k=-\infty}^{\infty} d_k^j \psi_k^j(x) \tag{6.24}$$

where the localized *little wave* functions $\psi_k^j(x)$

$$\psi_k^j(x) = 2^{-j/2}\psi(2^{-j}x - k) \tag{6.25}$$

are generated by the translations and dilations of the mother wavelet $\psi(x)$ on the dyadic grid. The integers $j, k \in \mathbb{Z}$ correspond to the scale and location of the center of the function, respectively.

One manifestation of the local nature of the set of functions $\{\psi_k^j(x)\}$ is their orthogonality across both scale and shift, i.e., they are chosen to satisfy

$$(\psi_k^j, \psi_{k'}^{j'}) = \int_{-\infty}^{\infty} \psi_k^j(x)\overline{\psi_{k'}^{j'}(x)}dx = \delta_{kk'}\delta_{jj'} \tag{6.26}$$

With the wavelet orthogonality property given by equation (6.26) the expansion, or wavelet, coefficients $\{d_k^j\}$ may be calculated directly by

$$d_k^j = \int_{-\infty}^{\infty} f(x)\overline{\psi_k^j(x)}dx \tag{6.27}$$

The direct application of this formula for the computation of the coefficients $\{d_k^j\}$ is generally avoided in favor of a much faster recursion scheme called multiresolution pyramidal decomposition, or *Mallat's algorithm* which is derived in general in Section 6.2.2. Note that the coefficient $d_k^j = X(b_k, a_j)$, i.e., it is the discretized CWT coefficient from Equation 6.23.

The wavelet expansion is local in the sense that only a few of the expansion coefficients $\{d_k^j\}$ contribute to the sum of the series $\sum_{j,k} d_k^j \psi_k^j(x)$ around any given point $x = x_o$. Note that the localization property of the expansion is

scale dependent and better time-localization is achieved for coefficients with small j, while better frequency localization is achieved for coefficients with large j.

Wavelet analysis on a dyadic grid is a form of *multi-resolution* analysis (MRA). The MRA procedes by splitting a function into nested subspaces of ever descreasing scale. The portion of the function which is removed at each level is projected into a wavelet subspace. With the MRA perspective, the construction of wavelets is based on first solving the *dilation* (or scaling) equation

$$\phi(x) = \sqrt{2}\sum h_k \phi(2x-k) \tag{6.28}$$

for the *scaling* function $\phi(x)$ The associated *wavelet* equation

$$\psi(x) = \sqrt{2}\sum g_k \phi(2x-k). \tag{6.29}$$

then produces the wavelet $\psi(x)$ associated with the MRA based on $\phi(x)$. A solution to the pair of equations (6.34) and (6.29) is constituted by appropriate coefficients $\{g_k\}$ and $\{h_k\}$ which determine the functions $\phi(x)$ and $\psi(x)$. The structure of the MRA determines the relationship between the g_k and the h_k and once the $\{h_k\}$ have been found the $\{g_k\}$ may be found in terms of them [81]. In addition, the Equation (6.34) is solved by determining appropriate coefficients $\{h_k\}$. These may then be used to find the scaling function $\phi(x)$ as described in Section 6.3. We shall see that the scaling function and associated wavelet derived from an MRA may or may not actually be determined in closed form.

Example 6.3. A simple example of a solution to the scaling Equation (6.34) is provided by the box function *box* function

$$\phi(x) = \begin{cases} 1 & \text{if } x \in [0,1), \\ 0 & \text{otherwise.} \end{cases} \tag{6.30}$$

with $h_0 = h_1 = 1/\sqrt{2}$. In other words,

$$\phi(x) = \phi(2x) + \phi(2x-1)$$

Example 6.4. The Haar wavelet

$$\psi(x) = \begin{cases} 1 & \text{if } x \in [0, \frac{1}{2}), \\ -1 & \text{if } x \in [\frac{1}{2}, 1), \\ 0 & \text{otherwise.} \end{cases} \tag{6.31}$$

provides a solution to the wavelet Equation (6.29) with $g_0 = 1/\sqrt{2}$ and $g_1 = -1/\sqrt{2}$.

Proposition 6.1. *The collection of translations and dilations of the Haar wavelet satisfy the orthonormality condition*

$$\int_{-\infty}^{\infty} \psi_k^j(x)\overline{\psi_{k'}^{j'}(x)}dx = \delta_{kk'}\delta_{jj'}$$

It is not hard to show this but we need some preliminary definitions.

Definition 6.1. *The support of a function $f(x)$, denoted supp$[f(x)]$, is the closure of the domain on which $f(x) \neq 0$.*

We shall first show that

$$\text{supp}[\psi_k^j(x)] = [2^j k, 2^j(k+1)].$$

To see this we apply the definition $\psi_k^j(x) = 2^{-j/2}\psi(2^{-j}x - k)$ which may be further evaluated as

$$\psi_k^j(x) = \begin{cases} 2^{-j/2} & \text{if } 2^{-j}x - k \in [0, \frac{1}{2}), \\ -2^{-j/2} & \text{if } 2^{-j}x - k \in [\frac{1}{2}, 1), \\ 0 & \text{otherwise.} \end{cases}$$

$$= \begin{cases} 2^{-j/2} & \text{if } x \in [2^j k, 2^j(k+\frac{1}{2})), \\ -2^{-j/2} & \text{if } x \in [2^j(k+\frac{1}{2}), 2^j(k+1)), \\ 0 & \text{otherwise.} \end{cases}$$

From this we conclude that two Haar wavelets at the same scale don't overlap, i.e.,

$$\text{supp}[\psi_k^j] \cap \text{supp}[\psi_{k'}^j] = \{\emptyset\}$$

At two different scales, $j \neq j'$, overlap is clearly possible. We leave it as an exercise to show that supp$[\psi_k^j] \subset$ supp$[\psi_{k'}^{j'}]$ where $j < j'$ and that $\psi_{k'}^{j'}(x) =$ constant for $x \in$ supp$[\psi_k^j]$. We can view this result graphically by considering the two functions

$$\psi_0^2(x) = \frac{1}{2}\psi(\frac{x}{4}) = \begin{cases} \frac{1}{2} & \text{if } x \in [0, 2), \\ -\frac{1}{2} & \text{if } x \in [2, 4), \\ 0 & \text{otherwise.} \end{cases}$$

and

$$\psi_1^0(x) = \psi(x-1) = \begin{cases} 1 & \text{if } x \in [1, \frac{3}{2}), \\ -1 & \text{if } x \in [\frac{1}{2}, 2), \\ 0 & \text{otherwise.} \end{cases}$$

To show that the Haar wavelet forms a basis for $L^2(\mathbb{R})$ it remains to show ψ_k^j are dense in $L^2(\mathbb{R})$, i.e., any $f \in L^2$ can be expressed as the superposition of the ψ_k^j to arbitrary precision. See [16] for a proof of this fact.

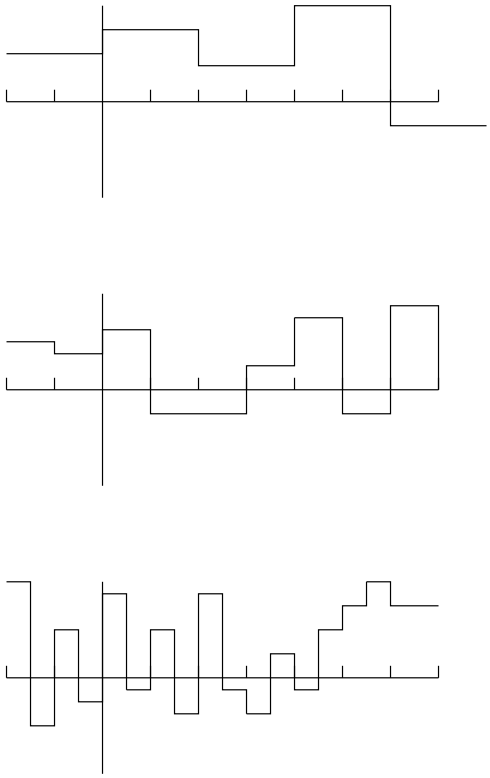

Fig. 6.8 Elements in different Haar subspaces.

6.2.1 The Multiresolution Property

The multiresolution analysis works by projecting a given function onto a sequence of subspaces $\ldots, V_{j-1}, V_j, V_{j+1}, \ldots$ of decreasing resolution.

The defining feature of the multiresolution analysis is the *multiresolution property.*

Property 6.2.1. *A sequence of subspaces*

$$\ldots, V_{j-1}, V_j, V_{j+1}, \ldots$$

possesses the multiresolution property (MRP) if for all j

$$f(x) \in V_j \leftrightarrow f(2x) \in V_{j-1} \tag{6.32}$$

Example 6.5. The sequence of *Haar* subspaces V_j where

$$V_j = \{f(x) \in L^2(\mathbb{R}) \,:\, f(x) = \text{constant on } x \in [2^j k, 2^j(k+1)),\ \forall k \in \mathbb{Z}\} \tag{6.33}$$

will serve as our primary example. The V_j are spanned by piecewise constant functions at different scales. For example,

$$V_0 = \{f(x) \in L^2(\mathbb{R}) \, : \, f(x) = \text{constant on } x \in [k, k+1), \forall k \in \mathbb{Z}\}$$

The Haar subspaces satisfy Property 6.32. We verify that $f(x) \in V_0 \Leftrightarrow f(2x) \in V_{-1}$. Given

$$f(x) \in V_0 \rightarrow f(x) = \text{constant for } x \in [k, k+1)$$

Since $f(2x) = \text{constant for } 2x \in [k, k+1)$ it follows

$$f(2x) = \text{constant for } x \in [\frac{k}{2}, \frac{k+1}{2})$$

therefore $f(2x) \in V_{-1}$.

It is this MRP which permits the construction of a bridge between the spaces $\{V_j\}$. The foundation for this bridge is the dilation of the basis for V_0: given a basis for V_0 we immediately have a basis for V_j.

Proposition 6.2. *Let $\{\phi_k^0 : k \in \mathbb{Z}\}$ be a basis for V_0. Then $\{\phi_k^j : k \in \mathbb{Z}\}$ is a basis for V_j.*

Proof. Since $\{\phi_k^0 : k \in \mathbb{Z}\}$ is a basis for V_0, any $q(x) \in V_0$ may be written $q(x) = \sum_k \alpha_k \phi(x-k)$. If $f(x) \in V_j$ then $f(2^j x) \in V_0$ by the MRP. Thus,

$$f(2^j x) = \sum_k \alpha_k \phi(x-k)$$

Setting $\xi = 2^j x$ we have

$$f(\xi) = \sum_k (\alpha_k 2^{j/2})(2^{-j/2})\phi(2^{-j}\xi - k)$$

or

$$f(\xi) = \sum_k \tilde{\alpha}_k \phi_k^j(\xi)$$

□

Example 6.6. If $\phi(x)$ is the box function, defined by Equation (6.30), then the translates of $\phi(x)$ are an orthonormal basis for V_0 as can be readily seen graphically.

Another basic property of the scaling spaces in our multiresolution analysis is nesting.

Property 6.2.2. *A sequence of subspaces is said to be nested if*

$$\cdots \subset V_{j+2} \subset V_{j+1} \subset V_j \subset V_{j-1} \subset V_{j-2} \subset \ldots$$

Example 6.7. The Haar subspaces V_j are nested. If $f(x) \in V_0$ then, by definition, $f(x)$ =constant for $x \in [k, k+1)$ so clearly $f(x)$ =constant for $x \in [\frac{k}{2}, \frac{k+1}{2})$, thus $V_0 \subset V_{-1}$. This example demonstrates a fundamental feature of the MRA. The coarser resolution subspace is a subset of the finer resolution subspace.

This nesting property satsified by the subspaces is the basis for one of the fundamental equations of the multiresolution analysis. In particular, if $V_0 \subset V_{-1}$ from which we obtain the *scaling*, or *dilation*, equation

$$\phi(x) = \sqrt{2} \sum h_k \phi(2x - k) \tag{6.34}$$

In the above equation it is assumed that $\{\phi_k^0\}$ is an o.n. basis for V_0. Thus, by the MRP $\{\phi_k^{-1}\}$ is an o.n. basis for V_{-1}. Finally, $\phi(x) \in V_0 \subset V_{-1}$.

As a consequence of the multiresolution Property 6.32, the scaling equation (6.34) and wavelet equation (6.29) relate not only V_0 and V_{-1} but also the adjacent subspaces V_j and V_{j-1}.

Proposition 6.3. *Given solutions to Equations (6.34) and (6.29) it follows that*

(i) $\phi_k^j(x) = \sum_k h_{m-2k} \phi_m^{j-1}(x)$

(ii) $\psi_k^j(x) = \sum_k g_{m-2k} \phi_m^{j-1}(x)$

Proof. Substituting $x = 2^{-j}\xi - k$ into the dilation equation we obtain

$$\phi(2^{-j}\xi - k) = \sqrt{2} \sum_l h_l \phi(2^{-j+1}\xi - 2k - l)$$

Letting $m = 2k + l$ it follows

$$\phi(2^{-j}\xi - k) = \sqrt{2} \sum_m h_{m-2k} \phi(2^{-(j-1)}\xi - m)$$

Proposition i) follows after multiplying both sides by $2^{-j/2}$. Proposition ii) may be shown in a similar manner. □

6.2.2 The Multiresolution Analysis

In this Section we demonstrate how the multiresolution property coupled with the nesting property may be used for efficient computation of the multiresolution decomposition and reconstruction of a function. In addition, we shall see that the multiresolution analysis framework provides a general procedure for constructing wavelets.

The spaces $\{V_j\}$ form a sequence of approximation spaces. The difference between the approximation from one level to the next resides in the *adjacent* wavelet space W_j. In general, the bases for the W_j are dictated by the bases for the V_j.

The wavelet subspace W_j is defined as the orthogonal complement to V_j in V_{j-1}, i.e.,

$$V_{j-1} = V_j \oplus W_j \tag{6.35}$$

and $W_j \perp W_j'$ if $j \neq j'$. Then the subspace V_j may be written

$$V_j = V_J \oplus W_J \oplus W_{J-1} \oplus \cdots \oplus W_{j+1} \tag{6.36}$$

where J denotes the coarsest resolution subspace. The remarkable aspect of this decomposition is the fact that we have the wavelet decomposition

$$L^2(\mathbb{R}) = \bigoplus_{j \in \mathbb{Z}} W_j. \tag{6.37}$$

Example 6.8. In this example it is demonstrated that the Haar wavelet is a basis for the difference between the Haar subspaces V_0 and V_{-1}. Define this Haar wavelet subspace as W_0 where

$$V_{-1} = V_0 \oplus W_0.$$

The function $\psi(x)$ which generates the basis for W_0 is constructed by the requirement that

$$(\phi(x), \psi(x)) = 0$$

which is satisfied if

$$\psi(x) = \phi(2x) - \phi(2x-1).$$

Thus the functions are orthogonal. They also provide the needed direct sum given the function $\phi(2x)$ which generates a basis for V_{-1} may be decomposed

$$\phi(2x) = \frac{\phi(x) + \psi(x)}{2}$$

We now define the projection operators P_j, Q_j such that for any $f(x) \in L^2(\mathbb{R})$

$$P_j f \in V_j \quad \text{and} \quad Q_j f \in W_j.$$

Then we have

$$\begin{aligned} P_{j-1} f(x) &= P_j f(x) + Q_j f(x) \\ f^{j-1}(x) &= f^j(x) + s^j(x) \end{aligned}$$

where $f^j \in V_j$ and $s^j \in W_j$. It is common to view P_j as a *low-pass* filter since it removes the finest scale and Q_j as a *high-pass* filter since all but the finest *detail* is removed. Specifically, we view s^j as the detail component of f^{j-1}.

As expansions we have

$$f^j(x) = P_j f(x) = \sum_{k \in \mathbb{Z}} c_k^j \phi_k^j(x) \tag{6.38}$$

where the $\{c_k^j\}$ are referred to as the *scaling* coefficients and

$$s^j(x) = Q_j f(x) = \sum_{k\in\mathbb{Z}} d_k^j \psi_k^j(x) \tag{6.39}$$

where the $\{d_k^j\}$ are referred to as the *wavelet* coefficients. Next we shall see how all of these coefficients may be calculated very efficiently using recursion once we are given the $\{c_k^j; \forall k \in \mathbb{Z}\}$ for some fixed resolution j.

To compute this first level of scaling coefficients we must in general perform a numerical integration. This is done using the identity

$$c_k^j = (f, \phi_k^j) = \int_{-\infty}^{\infty} f(x) 2^{-j/2} \phi(2^{-j}x - k) dx$$

Example 6.9. For the Haar wavelet we have

$$\phi(2^{-j}x - k) = \begin{cases} 1 & \text{if } x \in [2^j k, 2^j(k+1)), \\ 0 & \text{otherwise.} \end{cases}$$

which gives

$$c_k^j = 2^{-j/2} \int_{2^j k}^{2^j(k+1)} f(x) dx.$$

6.2.3 The Pyramidal Decomposition

Given the scaling coefficients $\{c_k^{j-1}; \forall k \in \mathbb{Z}\}$ for some fixed resolution j we seek *simple* expressions for $\{c_k^j\}$ and $\{d_k^j\}$.

Scaling Coefficient Recursion. To determine a recursion relation for the scaling coefficients first write

$$c_k^j = (f, \phi_k^j)$$

by Proposition 6.3 part i) this becomes

$$\begin{aligned} &= (f, \sum_m h_{m-2k} \phi_m^{j-1}) \\ &= \sum_m h_{m-2k} (f, \phi_m^{j-1}) \end{aligned}$$

Hence we have the desired recursion

$$c_k^j = \sum_m h_{m-2k} c_m^{j-1} \tag{6.40}$$

Example 6.10. For the Haar scaling function with $h_0 = h_1 = 1/\sqrt{2}$ the recursion formula becomes

$$c_k^j = \frac{c_{2k}^{j-1} + c_{2k+1}^{j-1}}{\sqrt{2}} \tag{6.41}$$

The coefficients at a given level j are seen to be *smoothed* versions of the coefficients at the higher resolution level $j-1$.

Wavelet Coefficient Recursion. To determine a recursion relation for the wavelet coefficients first write

$$d_k^j = (f, \psi_k^j)$$

by Proposition 6.3 part ii) this becomes

$$\begin{aligned} &= (f, \sum_m g_{m-2k} \psi_m^{j-1}) \\ &= \sum_m g_{m-2k} (f, \psi_m^{j-1}) \end{aligned}$$

Hence we have the desired recursion

$$d_k^j = \sum_m g_{m-2k} c_m^{j-1} \tag{6.42}$$

Example 6.11. For the Haar wavelet $g_0 = 1/\sqrt{2}$ and $g_1 = -1/\sqrt{2}$ Thus the recursion equation for the wavelet coefficients is given by

$$d_k^j = \frac{c_{2k}^{j-1} - c_{2k+1}^{j-1}}{\sqrt{2}}. \tag{6.43}$$

We see that for the Haar case that the wavelet coefficients are produced by differencing the scaling coefficients.

6.2.4 The Pyramidal Reconstruction

Now we derive the recursion relations going the other way. That is, we start with the function at its coarsest level and add on the detail from each of the wavelet subspaces. At each level we have

$$\begin{aligned} f^{j-1}(x) &= f^j(x) + s^j(x) \\ &= \sum_k c_k^j \phi_k^j(x) + \sum_k d_k^j \psi_k^j(x) \end{aligned}$$

$$\begin{aligned} c_n^{j-1} &= (f^{j-1}, \phi_n^{j-1}) \\ &= (\sum_k c_k^j \phi_k^j + \sum_k d_k^j \psi_k^j, \phi_n^{j-1}) \\ &= \sum_k c_k^j (\phi_k^j, \phi_n^{j-1}) + \sum_k d_k^j (\psi_k^j, \phi_n^{j-1}) \end{aligned}$$

Now we have all we need to evaluate the inner products above, i.e.,

$$\begin{aligned} (\phi_k^j, \phi_n^{j-1}) &= (\sum_m h_{m-2k} \phi_m^{j-1}, \phi_n^{j-1}) \\ &= \sum_m h_{m-2k} \delta_{mn} \\ &= h_{n-2k} \end{aligned}$$

Using the same approach it can also be shown that

$$(\psi_k^j, \phi_n^{j-1}) = g_{n-2k}.$$

Thus we have the general reconstruction formula

$$c_n^{j-1} = \sum_k h_{n-2k} c_k^j + \sum_k g_{n-2k} d_k^j \tag{6.44}$$

Example 6.12. *Haar Multiresolution Analysis.* We are now in the position to compute a wavelet decomposition of a function. We take as an example the decomposition of the vector $f = (9, 1, 2, 0)$ treated in detail in Strang's paper [81]. Our presentation stresses somewhat different points.

So how do we compute the $\{c_k^j\}$ and $\{d_k^j\}$ for this f? We start by viewing $f \in V_j$ where the V_j are the Haar multiresolution nested subspaces. We need to arbitrarily specify the size of the smallest scale to start the pyramidal decomposition algorithm. We will choose $\dim f = 4 = 2^{-j}$. Thus the finest resolution required is at the level V_{-2}.

Hence we view f as

$$f(x) = \begin{cases} 9 & \text{if } x \in [0, \frac{1}{4}), \\ 1 & \text{if } x \in [\frac{1}{4}, \frac{1}{2}), \\ 2 & \text{if } x \in [\frac{1}{2}, \frac{3}{4}), \\ 0 & \text{if } x \in [\frac{3}{4}, 1). \end{cases}$$

We will see that the decomposition in this case will involve the subspaces

$$V_{-2} = \text{span } \{2\phi(4x - k); k \in \mathbb{Z}\}$$

$$V_{-1} = \text{span } \{\sqrt{2}\phi(2x - k); k \in \mathbb{Z}\}$$

$$V_0 = \text{span } \{\phi(x-k); k \in \mathbb{Z}\}$$

where the coefficients normalize the functions such that orthonormal.

At the finest resolution, $j = -2$, the scaling coefficients $\{c_k^j\}$ are found by projecting f onto the basis for V_{-2}. I.e., since $P_{-2}f \in V_{-2}$ we write

$$P_{-2}f(x) = \sum_{k\in\mathbb{Z}} c_k^{-2}\phi_k^{-2}(x)$$

where

$$c_k^j = 2^{-j/2}\int_{2^j k}^{2^j(k+1)} f(x)dx$$

From which we have

$$c_k^{-2} = (f, \phi_k^{-2}) = 2\int_{k/4}^{(k+1)/4} f(x)dx.$$

Evaluating the integrals

$$c_0^{-2} = \frac{9}{2},\ c_1^{-2} = \frac{1}{2},\ c_2^{-2} = 1,\ c_3^{-2} = 0.$$

Also, $c_k^{-2} = 0$ for $k < 0, k > 3$.

Now project f onto V_{-1} via $P_{-1}f(x)$ and onto W_{-1} via $Q_{-1}f(x)$. We have

$$P_{-1}f(x) = \sum_k c_k^{-1}\phi_k^{-1}(x)$$

where using the recursion equation (6.41)

$$c_k^{-1} = \frac{1}{\sqrt{2}}(c_{2k}^{-2} + c_{2k+1}^{-2})$$

we get

$$c_0^{-1} = \frac{1}{\sqrt{2}}(c_0^{-2} + c_1^{-2}) = \frac{5}{\sqrt{2}}$$

$$c_1^{-1} = \frac{1}{\sqrt{2}}(c_2^{-2} + c_3^{-2}) = \frac{1}{\sqrt{2}}$$

and $c_2^{-1} = c_3^{-1} = 0$. Therefore,

$$\begin{aligned} P_{-1}f(x) &= c_0^{-1}\phi_0^{-1}(x) + c_1^{-1}\phi_1^{-1}(x) \\ &= 5\phi(2x) + \phi(2x-1) \end{aligned}$$

The *detail* is given by

$$Q_{-1}f(x) = \sum_k d_k^{-1}\psi_k^{-1}(x)$$

where $\psi(x)$ is the Haar wavelet. Using equation (6.43) at the level $j = -2$

$$d_k^{-1} = \frac{1}{\sqrt{2}}(c_{2k}^{-2} - c_{2k+1}^{-2}).$$

Hence

$$d_0^{-1} = \frac{1}{\sqrt{2}}(c_0^{-2} - c_1^{-2}) = \frac{4}{\sqrt{2}}$$

$$d_1^{-1} = \frac{1}{\sqrt{2}}(c_2^{-2} - c_3^{-2}) = \frac{1}{\sqrt{2}}$$

Therefore,

$$\begin{aligned} Q_{-1}f(x) &= d_0^{-1}\psi_0^{-1}(x) + d_1^{-1}\psi_1^{-1}(x) \\ &= \frac{4}{\sqrt{2}}\psi_0^{-1} + \frac{1}{\sqrt{2}}\psi_1^{-1} \end{aligned}$$

We can write these in terms of the box function using the relations

$$\psi_0^{-1} = \frac{1}{\sqrt{2}}(\phi_0^{-2} - \phi_1^{-2}) = \frac{1}{\sqrt{2}}(2\phi(4x) - 2\phi(4x-1))$$

and

$$\psi_1^{-1} = \frac{1}{\sqrt{2}}(\phi_2^{-2} - \phi_3^{-2}) = \frac{1}{\sqrt{2}}(2\phi(4x-2) - 2\phi(4x-3))$$

Thus we have the projection onto W_{-1} as

$$Q_{-1}f(x) = 4(\phi(4x) - \phi(4x-1)) + (\phi(4x-2) - \phi(4x-3)).$$

which is the portion of $f(x)$ contained in the wavelet subspace at level $j = -1$.

The projection onto V_0 proceeds similarly via the computation of $P_0 f(x)$. The scaling coefficients at the level $j = 0$ are found using

$$c_k^0 = \frac{1}{\sqrt{2}}(c_{2k}^{-1} + c_{2k+1}^{-1})$$

The single non-zero scaling coefficient is given by

$$c_0^0 = \frac{1}{\sqrt{2}}(c_0^{-1} + c_1^{-1}) = 3$$

and the associated wavelet coefficient is

$$d_0^0 = \frac{1}{\sqrt{2}}(c_0^{-1} - c_1^{-1}) = 2.$$

Now we have

$$P_0 f(x) = c_0^0 \phi_0^0(x) = 3\phi(x)$$

and

$$\begin{aligned} Q_0 f(x) &= d_0^0 \psi_0^0(x) \\ &= 2(\frac{1}{\sqrt{2}}(\phi_0^{-1} - \phi_1^{-1})) \\ &= \frac{2}{\sqrt{2}}(\sqrt{2}\phi(2x) - \sqrt{2}\phi(2x-1)) \\ &= 2(\phi(2x) - \phi(2x-1)) \end{aligned}$$

Note, $f(x) \in V_{-2}$ without approximation. In summary,

$$\begin{aligned} f(x) &= P_{-2} f(x) \in V_{-2} \\ &= P_{-1} f(x) + Q_{-1} f(x) \in V_{-1} \oplus W_{-1} \\ &= P_0 f(x) + Q_0 f(x) + Q_{-1} f(x) \in V_0 \oplus W_0 \oplus W_{-1} \end{aligned}$$

6.2.5 The Multiresolution Theorem

To this point we have simply assumed that the scaling function $\phi(x)$ and the associated wavelet $\psi(x)$ exist. Now we specify the circumstances under which this is true.

A *multiresolution analysis* consists of a sequence of closed subspaces with the following six properties:

Property 6.2.3. *Each subspace is a scaled replica of the other*

$$f(x) \in V_j \Leftrightarrow f(2x) \in V_{j-1} \tag{6.45}$$

Property 6.2.4. *The subspaces are nested*

$$\cdots \subset V_2 \subset V_1 \subset V_0 \subset V_{-1} \subset V_{-2} \subset \ldots \tag{6.46}$$

Property 6.2.5. *The closure of the subspaces is identified with all square integrable functions*

$$\overline{\bigcup_{j \in \mathbb{Z}} V_j} = L^2(\mathbb{R}) \tag{6.47}$$

Property 6.2.6. *The intersection of the subspaces contains only zero*

$$\bigcap_{j \in \mathbb{Z}} V_j = \{0\} \tag{6.48}$$

Property 6.2.7. *The subspace V_0 is invariant under integer translations,*

$$f(x) \in V_0 \rightarrow f(x-k) \in V_0 \ \ \forall k \in \mathbb{Z}. \tag{6.49}$$

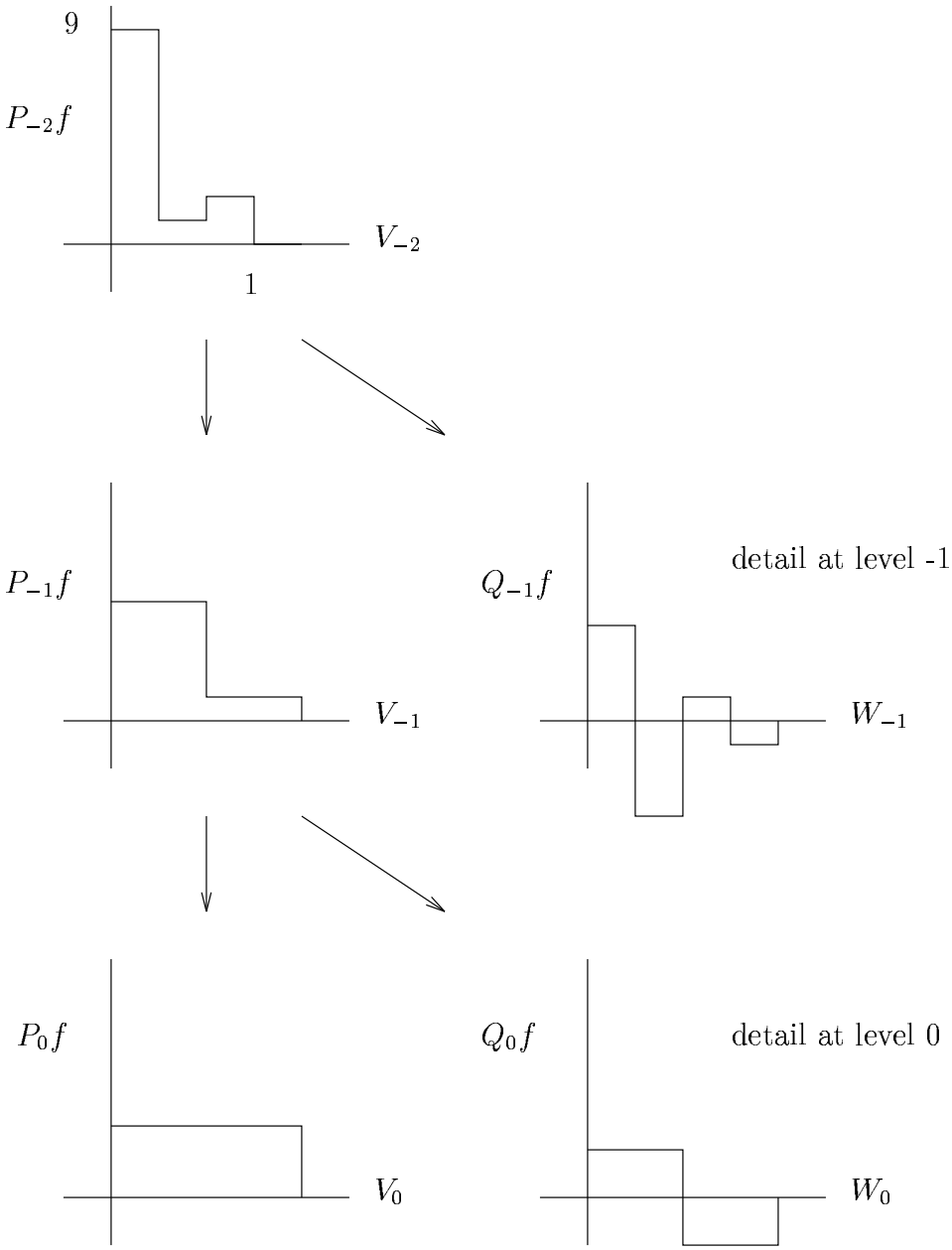

Fig. 6.9 The wavelet decomposition.

Property 6.2.8. *There exists a scaling function $\phi(x)$ s.t. $\{\phi(x-k); \forall k \in \mathbb{Z}\}$ is an o.n. basis in V_0.*

The power of a multiresolution analysis is that it expresses a function $f \in L^2(\mathbb{R})$ as a limit of successive approximations with increasing resolution. Furthermore, if the above axioms hold for a sequence $\{V_j\}$ then there is always an associated wavelet $\psi(x)$ which acts as the o.n. basis for the W_j.

Theorem 6.1. *If a sequence of closed subspaces V_j of $L^2(\mathbb{R})$ satsify Properties 6.2.3-6.2.8, then there exists an associated wavelet*

$$\psi(x) = \sqrt{2}\sum_n (-1)^{n-1} h_{-n-1}\phi(2x-n)$$

which generates bases $\psi_k^j(x)$ for W_j. Furthermore,

$$P_{j-1}f = P_j f + \sum_{k\in\mathbb{Z}} d_k^j \psi_k^j. \tag{6.50}$$

The proof of this theorem may be found, e.g., in [16].

By the completeness property we have

$$\lim_{j\to-\infty} P_j f = f. \tag{6.51}$$

6.3 THE DILATION EQUATION

One of the main approaches for constructing a multiresolution analysis is to determine the scaling function $\phi(x)$ which satisfies the dilation equation

$$\phi(x) = \sqrt{2}\sum_{k\in\mathbb{Z}} h_k \phi(2x-k)$$

with appropriate side constraints. For example, a particularly attractive solution $\phi(x)$ will generate an o.n. family directly. It is possible, as we shall see, to compute solutions which do not have this property. In these cases the orthonormality must be achieved via an orthogonalization trick. Although the penalty of applying the orthonormalization procedure is that the resulting o.n. family no longer has compact support. Any solution $\phi(x)$ associated with a finite number of non-zero $\{h_k\}, k = 0..N$ will have support on the compact interval $[0, N]$.

6.3.1 Iteration of the Dilation Equation

Consider the algorithm

$$\phi^{(n)}(x) = \sqrt{2}\sum_{k=0}^{N} h_k \phi^{(n-1)}(2x-k) \tag{6.52}$$

where $\phi^{(0)}(x) \in L^1$, in particular $\int \phi^{(0)}(x) = 1$.

Proposition 6.4. *If the scaling function $\phi(x) \in L^2$ exists for the coefficients $\{h_k\}$ then the cascade algorithm will converge to it, i.e.,*

$$\phi(x) = \lim_{n \to \infty} \phi^{(n)}(x)$$

Support of the Scaling Function. The above iteration algorithm provides a method to compute the support of the scaling function $\phi(x)$ associated with a finite length filter.

Proposition 6.5. *If the solution to the scaling equation has all zero coefficients except possibly for $\{h_k\}$ where $k = 0, \ldots, N$ then $supp(\phi(x)) = [0, N]$.*

6.3.2 Constraints on the coefficients $\{h_k\}$

Normalization of $\phi(x)$. By convention we require that the scaling function be normalized according to

$$\int_{-\infty}^{\infty} \phi(x)dx = 1 \tag{6.53}$$

In practice it is sufficient that the right-hand side be non-zero and finite. As we shall see, this restriction ensures that for a given collection of coefficients $\{h_k\}$ there is a unique $\phi(x)$. Hence, we may view a solution of the dilation equation to consist of these coefficients which uniquely determine the scaling function as long as equation (6.53) holds.

The properties and constraints of the scaling function readily translate into equations involving the coefficients $\{h_k\}$. The normalization constraint given in equation (6.53) provides us with our first example. Integrating the dilation equation

$$\int \phi(x)dx = \sqrt{2} \sum_{k \in \mathbb{Z}} h_k \int \phi(2x - k)dx$$

Letting $x' = 2x - k$ and substituting equation (6.53) gives

$$1 = \sqrt{2} \sum_{k} h_k \int \phi(x') \frac{dx'}{2}$$

After substituting equation (6.53) again, we obtain the normalization property in terms of the filter coefficients

$$\sum_{k \in \mathbb{Z}} h_k = \sqrt{2} \tag{6.54}$$

Othogonality Constraint on $\phi(x)$. The orthogonality of the $\phi(x-k)$ gives another condition that the $\{h_k\}$ must satisfy. Again, given

$$\phi(x) = \sqrt{2}\sum_k h_k \phi(2x-k)$$

the translates may be represented as

$$\phi(x-m) = \sqrt{2}\sum_k h_k \phi(2x-2m-k).$$

Substituting these equations into the orthogonality condition

$$\int \phi(x)\phi(x-m)dx = \delta_{0m}$$

we have

$$\begin{aligned}\int \phi(x)\phi(x-m)dx &= \int \sqrt{2}\sum_k h_k \phi(2x-k)\sqrt{2}\sum_{k'} h_{k'}\phi(2x-2m-k')dx \\ &= 2\sum_{kk'} h_k h_{k'} \frac{\delta_{k,2m+k'}}{2}\end{aligned}$$

Thus the orthogonality property of the scaling function is expressed in terms of the coefficients solving the dilation equation as

$$\sum_k h_k h_{k-2m} = \delta_{m0}. \tag{6.55}$$

Note that out of all the previous examples, only the Haar scaling function satisfies the o.n. constraint.

Zero Moment Constraints on $\psi(x)$. In addition, we may apply constraints to these coefficients g_k, h_k which impact the properties of the wavelet expansion. In fact, the number of vanishing moments p of $\psi(x)$, i.e.,

$$\int_{-\infty}^{\infty} x^m \psi(x)dx = 0$$

for $m = 0, \ldots, p-1$ determines the order of accuracy of the wavelet expansion. The Haar wavelet is not appropriate for many applications due to the fact it is not smooth, and low order of accuracy of its approximations (it has only one vanishing moment). However, it is an excellent introductory example and many of the ideas central to wavelet analysis are readily apparent in the context of the Haar wavelet.

The following theorem from [81] relates how the number of zero moments of the wavelet basis is formulated as a condition on the $\{h_k\}$.

Theorem 6.2. *Let $\phi(x)$ and $\psi(x)$ be a scaling and wavelet function which generate an MRA $\{V_j\}$ as well as the orthogonal subspaces W_j. Then*

$$\int x^m \psi(x) dx = 0$$

for $m = 0, \ldots, p-1$ iff

$$\sum_k (-)^k k^m h_k = 0$$

The proof of this theorem (see [81]) requires that $\phi(x)$ and $\psi(x)$ decay faster than $O(|x|^{-m-1})$. In practice this is no problem since $\phi(x)$ and $\psi(x)$ have either compact support or decay exponentially.

Furthermore, if the above theorem holds for $m = 0, 1, \ldots, p-1$, then

- $1, x, \ldots, x^{p-1}$ are spanned by the $\{\phi(x-k)\}$.
- $O(h^p)$ accuracy, i.e.,

$$\|f(x) - \sum_k a_k \phi(2^j x - k)\| \leq C 2^{-jp} \|f^{(p)}\|$$

- The wavelet coefficients decay as

$$|d_k^j| \leq C 2^{-jp} \|f^{(p)}\|$$

6.3.3 Solutions of the Scaling Equation

Example 6.13.

$$h_0 = \frac{1}{2\sqrt{2}}, \quad h_1 = \frac{1}{\sqrt{2}}, \quad h_2 = \frac{1}{2\sqrt{2}}$$

and the remaining $h_j = 0, \ \forall j \neq \{0, 1, 2\}$. This scaling function corresponds to an equilateral triangle of unit height of width 2, centered at $x = 1$. This does not directly produce an o.n. family.

Example 6.14.

$$h_0 = \frac{1}{4}, \quad h_1 = h_2 = \frac{3}{4}, \quad h_3 = \frac{1}{4}$$

and the remaining $h_j = 0, \ \forall j \neq \{0, 1, 2, 3\}$. This scaling function corresponds to the quadratic cardinal B-spline. It has support $[0, 3]$ and does not directly produce an o.n. family.

Example 6.15. *Daubechies Compactly Supported Orthonormal Wavelets.* The main drawback of the Haar wavelet is that it is not smooth.

$$h_0 = \frac{1+\sqrt{3}}{4\sqrt{2}}, \quad h_1 = \frac{3+\sqrt{3}}{4\sqrt{2}}, \quad h_2 = \frac{3-\sqrt{3}}{4\sqrt{2}}, \quad h_3 = \frac{1-\sqrt{3}}{4\sqrt{2}} \tag{6.56}$$

and the remaining $h_j = 0, \ \forall j \neq \{0,1,2,3\}$ The corresponding function $\phi(x)$ has compact support $[0,3]$ and produces an o.n. family and compactly supported wavelets. It is continuous but only weakly differentiable.

Problems

6.1 Derive Equation (6.13).

6.2 Show Proposition (6.6).

6.3 Prove Proposition (6.1.5).

6.4 Find the CWT of $x(t) = \cos(\omega_0 t) + \delta(t - t_0)$.

6.5 Derive the condition given by equation (6.20) which determines the influence of an interval of frequencies on the value CWT $X(b,a)$ at the point (b_0, a_0). Draw this region of influence in the (b,a)-plane.

6.6 This problem concerns computing the maximum value of the magnitude of $X(b,a)$ for an input signal of the form $x(t) = \exp(i\omega_0 t)$. For simplicity assume that $a, \omega_0 > 0$

a) Show that for the mexican hat wavelet $\psi(t) = \frac{2}{\sqrt{3}}\pi^{-\frac{1}{4}}(1-t^2)\exp(-t^2/2)$ that the value of a corresponding to a peak in the transform is given by $a = \frac{1}{\omega_0}\sqrt{\frac{5}{2}}$.

b) Show that for Morlet's wavelet $\psi(t) = \frac{1}{\sqrt{2\pi}}\exp(i\alpha t - t^2/2)$ that $a = \frac{1}{2\omega_0}(\alpha + \sqrt{\alpha^2+2})$.

6.7 A wavelet is said to be progressive if its Fourier transform has the property that

$$\tilde{\psi}(\omega) = 0 \quad if \quad \omega < 0$$

Consider the signal $x(t) = \sin(\omega_0 t)$. Show that if the CWT $X(b,a)$ of this signal is computed using a progressive wavelet then the magnitude of the CWT $|X(b,a)|$ is independent of b.

6.8 *Constant Q analysis.* Assume that the Fourier transform of a wavelet has finite bandwidth which is non-zero on the interval $\omega \in [\omega_{\min}, \omega_{\max}]$. Noting that the width of the window is a function of the scale a of the wavelet and that the center frequency may be defined as geometric mean of the edges of the window compute the (*constant*) Q, or *quality* factor of the CWT defined as

$$Q = \frac{\text{center frequency}}{\text{bandwidth}}$$

The wavelet transform is often referred to as constant Q frequency analysis.

6.9 Compute by hand the Haar wavelet decomposition of the vector $\mathbf{x}^T = (1, 7, -3, 2)$ and graphically show the projections onto the scaling and wavelet subspaces.

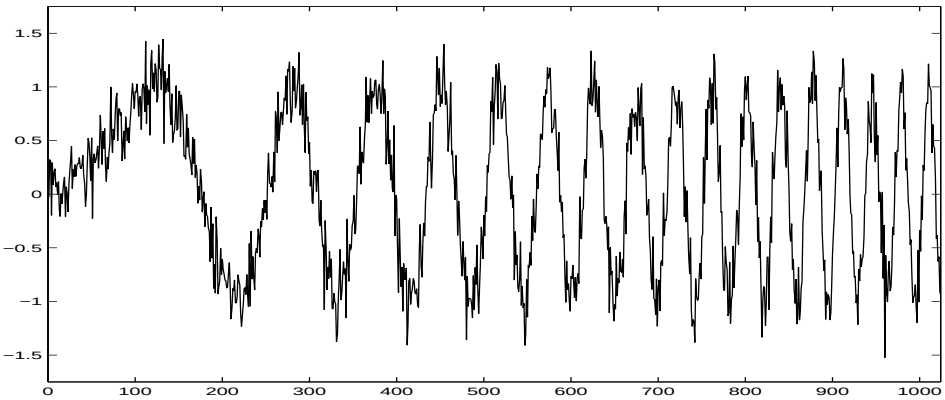

Fig. 6.10 Data corresponding to Equation (6.57). See computer project 6.11.

Computer Projects

6.10 Write a computer code to implement the discretization of the CWT as described in Section 6.1.2. Compute the approximate CWT by evaluating the integrals numerically using Simpson's rule with a step size of $h = .01$. Find the CWT of $x(t) = \sin(5t) + \sin(\sqrt{26}t)$ and compare with the analytically calculated result. In this problem you may employ either Morlet's wavelet or the mexican hat wavelet. Take $\alpha = 2^{1/12}, \beta = 1$ and compute $|X(b_k^j, a_j)|$ for enough scales and time steps to develop a good picture of the scalogram.

6.11 Write a computer code to implement the Haar wavelet transform including the algorithms for

- Haar pyramidal decomposition
- Haar pyramidal reconstrcution

Compute the 6 level decomposition of the data

$$f_n = \sin(\frac{n^2}{10000}) + \eta_n \tag{6.57}$$

where $n = 1, \ldots, 1024$, η_n is selected from a normal distribution with mean zero and variance 0.2. Initialize the transform by assuming that $\mathbf{f} \in V_0$, i.e., the function is constant over unit intervals. Include the following bar plots in your report:

a) $\mathbf{f}^1 \in V_1, \mathbf{f}^2 \in V_2, \mathbf{f}^3 \in V_3, \mathbf{f}^4 \in V_4$

b) $\mathbf{s}^1 \in W_1, \mathbf{s}^2 \in W_2, \mathbf{s}^3 \in W_3, \mathbf{s}^4 \in W_4$

Be sure that each bar plot has domain $[1, 1024]$.

Part IV

Adaptive Nonlinear Mappings